https://doi.org/10.1016/j.nanoen.2021.106672

Scalable Core–spun Coating Yarn-based Triboelectric Nanogenerators with Hierarchical Structure for Wearable Energy Harvesting and Sensing via Continuous Manufacturing

Yuanyuan Gao, Zihua Li, Bingang Xu*, Meiqi Li, Chenghanzhi Jiang, Xiaoyang Guan, Yujue Yang

Nanotechnology Center, Institute of Textiles and Clothing, The Hong Kong Polytechnic University, Hung Hom, Kowloon, Hong Kong, China

*Corresponding author; Email: tcxubg@polyu.edu.hk

Abstract

With rapid advancement in wearable electronics, textile-based triboelectric nanogenerators (T-TENGs) have attracted great attention for energy harvesting and bio-motion sensing because of their softness, lightweight, and comfort properties. However, the interface bonding between functional materials and textile substrate, and the compatibility with manufacturing still face considerable challenges. Herein, a kind of scalable core–spun coating yarn-based triboelectric nanogenerators (CSCY-TENGs) with a hierarchical architecture is designed and developed via continuous manufacturing which integrates yarn spinning, coating and braiding technologies to achieve fully continuous production. In this method, spinning technology was used to spin a kind of conductive core-spun yarns with silver-plated nylon yarn (SNY) as core and insulating cotton fibers as shell, where SNY serves as electrode and cotton fibers serve as base materials for absorbing/coating with triboelectric materials. Then multiple core-spun yarns coated with nylon and doped polydimethylsiloxane are used as positive and negative triboelectric materials to realize hierarchical CSCY-TENGs by braiding technology. The CSCY-TENGs can be washed and compatible with industrial-scale manufacturing. Besides, it can achieve an output voltage of 174 V, and a peak power density and an average power density of 275 mW/m^2 and 57 mW/m^2 respectively. As demonstration, the CSCY-TENG can charge various commercial capacitors and power low-power electronics. It can also be used as an anti-theft alarm carpet and energy harvesting shoes for bio-motion detection and energy harvesting.

Keywords: Triboelectric Nanogenerator; Energy Harvesting; Core-spun Coating Yarn; Interface Bonding; Intelligent Textiles

1. Introduction

The rapid development of wearable electronics has urgent demands on sustainable and stable power supplies. Traditional energy storage devices such as rigid batteries and electrochemical supercapacitors are becoming more and more unfavorable due to the inherent shortcomings of limited lifetime cycles, high recharging costs, potential safety risks and environmental hazards[1-3]. Recently, energy harvesting techniques that harvest and generate electricity directly from the surroundings are promising approaches to address these above problems[4-6]. Among them, triboelectric nanogenerator (TENG)[7] based on the coupling effect of contact electrification and electrostatic induction has become a promising technology, which can convert mechanical energy into electrical energy[8]. Owing to high efficiency, light weight, environmental friendliness and simple fabrication[9, 10], TENG is generally regarded as a promising solution for energy harvesting equipment and active sensors. Textile-based triboelectric nanogenerators (T-TENGs) have not only attracted the attention of scientific researchers, but also the industries in smart and functional wearables. They are considered to be the main direction of future textile development[7, 11-13]. The development of T-TENGs have turned traditional rigid devices into soft[14], light, durable and comfortable devices with not only sensing functions[15], but also responsive functions[16]. T-TENGs provide a more effective way to harvest energy from human motions because of its unique wearable properties. The notable T-TENG was reported by Zhong et al[17]. It is composed of two entangled modified-cotton threads, which exploits the biomechanical motions/vibration energy as natural energy sources for mobile medical systems. Jung et al.[18], Zhou et al. [19]and Pu et al. [20] also made related research on the first-generation of T-TENGs.

In recent years, T-TENGs have received widespread attention owing to its flexibility, good performance and promising potentials in medical and health observation[20-24], safety monitoring[25, 26], and human motion detection[27-30]. T-TENGs provide a feasible and convenient approach for the integration of fibers, yarns and fabrics[1, 3, 31] with functional components for self-powered sensing[32-34], energy harvesting and storage[35, 36]. The application of T-TENGs in the textile industry provides exciting potential for energy textiles. Traditional textile materials usually suffer from limited electrical outputs due to their inherent physicochemical properties[37]. A common strategy for improving the electrical performance of T-TENG is to introduce desired functional materials onto the textiles and enhance its triboelectric performance

by improving their surface charge density, thereby enhancing the electrical output of T-TENG. However, most electrodes used in T-TENG are conductive metal wires or metal plated yarns[38, 39], which have smooth surfaces and high surface energy, resulting in poor adsorption and interfacial incompatibility with polymeric triboelectric materials. Considering the scalable production of T-TENG, a simplified, efficient and steady method is highly desired for the integration of triboelectric materials with the textiles[40-43].

Herein, a kind of core–spun coating yarn-based triboelectric nanogenerators (CSCY-TENGs) with a hierarchical architecture is designed and developed via continuous manufacturing which integrates yarn spinning, coating and braiding technologies to achieve fully mechanized continuous production. We first use conventional textile spinning technology to spin a kind of conductive core-spun yarns with conductive silver-plated nylon yarn (SNY) as core and insulating cotton staple fibers as shell. For the core-spun yarns, the SNY serves as electrode and cotton staple fibers serve as base materials for absorbing/coating with good triboelectric materials. Then core-spun yarns are coated with nylon as positive triboelectric materials and doped polydimethylsiloxane (PDMS) as negative triboelectric materials, respectively with coating technology and equipment. The core-spun yarn utilizes the good absorbability and compatibility of cotton fibers with organic triboelectric materials and the strong wrapping force of cotton fibers on the surface of conductive yarns for essentially enhancing the interface bonding of triboelectric materials with conductive yarns. Finally, multiple nylon coated core-spun yarns (N-ccsys) are braided together with multiple doped PDMS coated core-spun yarns (P-ccsys) by braiding technology with polyvinyl alcohol (PVA) as a sacrificed material around N-ccsys. By dissolving the PVA, CSCY-TENG with a hierarchical architecture is realized with N-ccsys as core and P-ccsys as shell. As demonstration, the CSCY-TENG can charge various commercial capacitors and power low-power electronics. It can also be used as an anti-theft alarm carpet and sustainable energy harvesting shoes for bio-motion detection and energy harvesting, respectively.

2. Results and discussion

Structural design of CSCY-TENG. The structural design and fabrication method of the CSCY-TENG are schematically illustrated in Fig. 1. First, SNY and cotton roving

are prepared and spun into conductive core-spun yarns by spinning technology on a ring machine, where the SNY serves as the conductive core and the cotton fibers serve as the insulating shell (Fig. 1a-b). Then the core-spun yarns are coated with nylon and PDMS doped with Barium Titanate nanoparticles (PDMS@$BaTiO_3$) to obtain the N-ccsy and P-ccsy, respectively (Fig. 1c) (see Fig. S1 in Supporting Information). For enhancing the electric performance, multiple N-ccsys are braided to form as the core of CSCY-TENG by braiding technology (Fig. 1d). Then, PVA is braided around the N-ccsys as a sacrificed layer which will be removed in a later stage in order to obtain a gap between N-ccsy and P-ccsy (Fig. 1e). Then, multiple P-ccsys are braided onto the PVA surface (Fig. 1f). Finally, the CSCY-TENGs are obtained after removing PVA with water (Fig. 1g). Fig. 1h and i show the cross-section SEM images of the N-ccsys and P-ccsy respectively, where the SNY is located in the center, nylon/PDMS@$BaTiO_3$ are distributed in the outer layer of coated core-spun yarns, and cotton fibers play an important role as the middle layer of core-spun yarns for the good adsorption/coating of nylon / PDMS@$BaTiO_3$ and the tightly wrapping force on the surface of conductive yarn, contributing to the enhanced interface bonding of triboelectric materials (organic with very low surface energy) with conductive yarns (metal with very high surface energy) (see Fig. S2 in Supporting Information). Besides, in order to confirm this adsorption capacity of coer-spun yarn, a comparison of direct coating on bare conductive yarns and a core-spun yarn coating strategy was performed. PDMS@ $BaTiO_3$ coated directly on bare conductive yarn is prone to form beads due to the poor interfacial compatibility between metal and polymer. In comparison, PDMS@ $BaTiO_3$ can be tightly wrapped on the core-spun yarns to form a continuous and smooth coating (see Fig. S3 in Supporting Information).

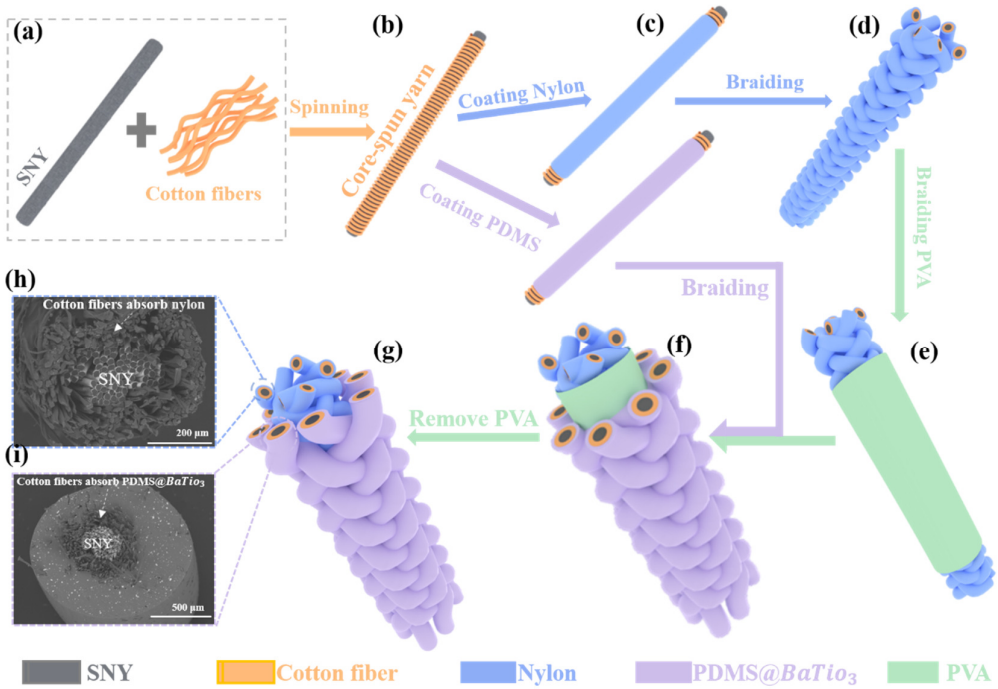

Fig. 1 Schematic diagram for structural design and fabrication method of the CSCY-TENG. (a-d) Fabrication processes of the core of CSCY-TENG. (e) PVA roving wrapping on the core of CSCY-TENG. (f) The CSCY-TENG before removing PVA. (g) Structural diagram of CSCY-TENG. Cross-sectional SEM images of (h) the N-ccsy (scale bar: 200 μm), and (i) the P-ccsy (scale bar: 500 μm).

Continuous manufacture of CSCY-TENG. The continuous manufacture of CSCY-TENG much depends on the continuity of the electrode, insulting staple fibers, triboelectric materials, spinning machine, coating equipment and braiding machine. In addition, the proper fineness of core-spun yarn, N-ccsy or P-ccsy determines the operability of the spinning and braiding machines. Based on the consideration of the above, spinning, coating and braiding machines have been employed, as schematically shown in Fig. 2. In order to obtain a good covering effect for the core-spun yarns, the spinning machine adds a filament guide device and combines a tension device to adjust the position of the core yarn (Fig. 2a). As shown in the enlarged twisted part, the SNY as the core yarn is located in the middle, and the cotton fibers as the shell will cover the SNY completely (see Fig. S4 and Video 1 in Supporting Information). Fig. 2b shows an equipment designed for continuous and scalable coating of the triboelectric materials. The reaction chamber and temperature sensor of the coating machine can provide a controllable temperature environment to completely cross-linking of the P-ccsy during the preparation process (see Fig. S5 and Video 2 in Supporting Information). In addition, in order to ensure the fineness of N-ccsy and P-ccsy, the machine adds a tubular hole to

scrape off excess liquid. Therefore, the fineness of the two coating yarns (i.e., N-ccsy and P-ccsy) is controlled within 1.2 mm before going into the next braiding machine. Fig. 2c and 2d show the schematic diagram and photograph of the braiding machine, respectively (see Fig. S6 and Video 3 in Supporting Information). Fig. 2e shows a partial enlarged photograph of the braided CSCY-TENG with a diameter of about 4 mm.

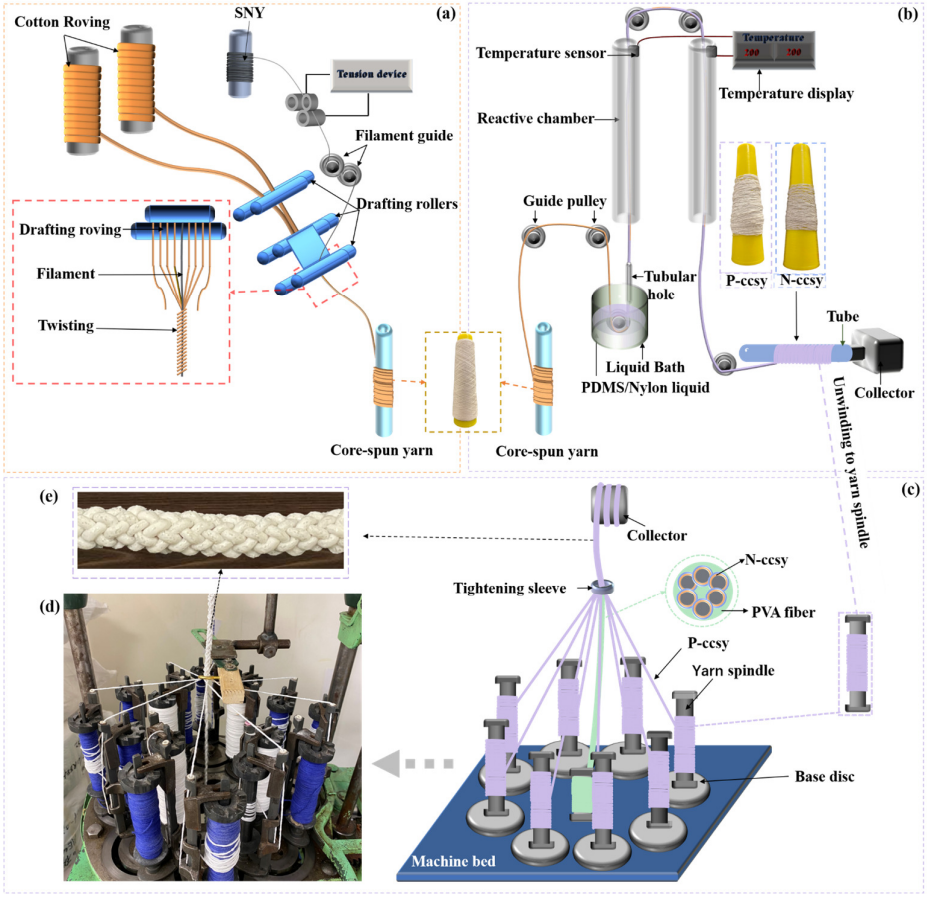

Fig. 2 Schematic diagrams for continuous manufacturing of CSCY-TENGs. (a) Ring machine for producing the core-spun yarns, (b) coating equipment for coating of core-spun yarns to make N-ccsy and P-ccsy. (c) Schematic diagram and (d) photograph of braided machine for producing the CSCY-TENGs. (e) Photograph of the CSCY-TENG

Working mechanisms of the CSCY-TENG. The working principle of the CSCY-TENG is illustrated in Fig. 3, which operates under a vertical contact and separation mode. Fig. 3a shows the photograph of an assembly of CSCY-TENGs with a size of 36 cm^2. Fig. 3b-c show the photograph of a single CSCY-TENG and the diagram of its cross-section composed of multiple N-ccsys and P-ccsys, respectively. In order to better and more intuitively understand the charge transfer process in the contact separation motion, the cross sections of a single N-ccsy and a single P-ccsy are demonstrated. The

compression and release movement of the whole cycle can be simplified as a contact separation process between the two coating yarns (Fig. 3d). When the CSCY-TENG is pressed (Fig. 3d-i), the negative triboelectric charges on the surface of P-ccsy are completely balanced by the positive electrostatic charges induced on the surface of N-ccsy. When the force is releasing (Fig. 3d-ii), the electrode of N-ccsy gradually induces positive charges to the electrode of P-ccsy under the electrostatic induction. The electric potential difference between two yarns will drive the reverse flow of electrons, which results in an instantaneous current. When the force is fully released (Fig. 3d-iii), P-ccsy and N-ccsy will be in the maximum separated state. The transfer of charge reaches an equilibrium state. If the CSCY-TENG is compressing (Fig. 3d-iv), the positive charges accumulated on the electrode of P-ccsy will flow back to the electrode of N-ccsy to compensate for the potential difference. The current in the opposite direction is formed until back to the pressed state (Fig. 3d-i). Therefore, alternating current is periodically generated with contact and separation process through external loads. To understand the power generation process, the potential distribution of constituent components is simulated using COMSOL Multiphysics software, as shown in Fig. 3e. Theoretical curves of short-circuit charge (Q_{sc}), open-circuit voltage (V_{oc}), and intrinsic capacitance (C) have been obtained. The Q_{sc} and V_{oc} increase with the increase of contact distance, and reach the maximum value at complete separation. According to the calculation of the intrinsic capacitance[8, 44], as the distance increases, the capacitance gradually decreases (see Fig. S7a-c in Supporting Information).

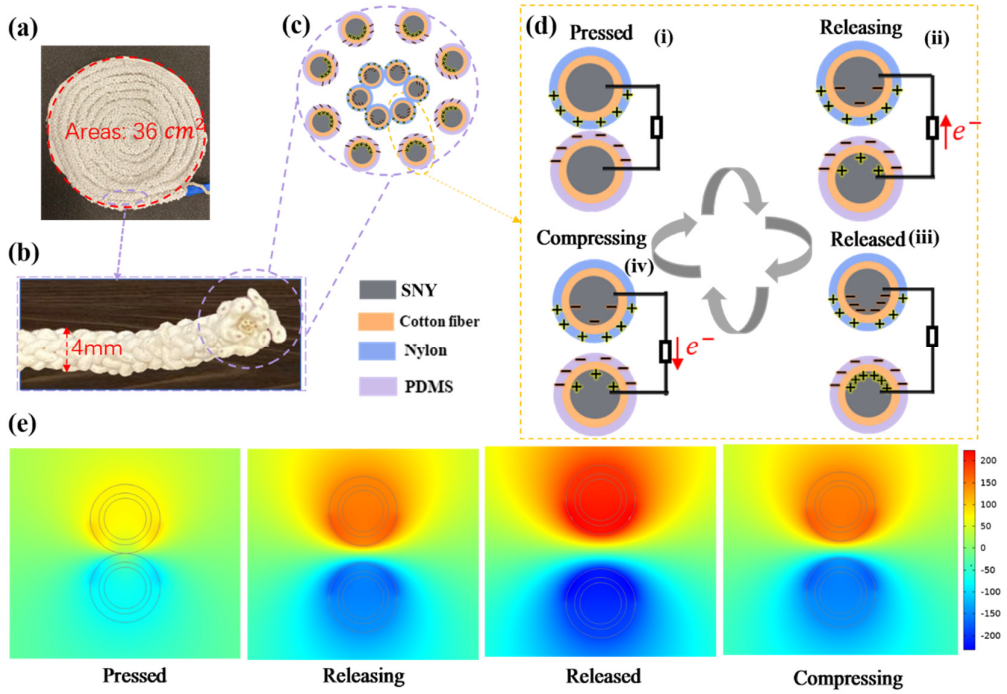

Fig. 3 The photographs of (a) CSCY-TENG with a size of 36 cm^2 and (b) a single CSCY-TENG with a diameter of about 4mm. (c) The schematic illustration of the cross-section of CSCY-TENG. (d) Electricity generation mechanisms of the CSCY-TENG in a vertical contact and separation mode. (e) Simulation results for potential distribution of constituent components by COMSOL.

Output performance evaluation of the CSCY-TENG. The output performance of the CSCY-TENG in vertical contact-separation mode is systematically studied. As shown in Fig. 4a and Fig. S8a in Supporting Information, at a given impact force of 50 N and a frequency of 4 Hz, the output voltage and Q_{sc} is increased from 75 V/41 nC to 135 V/120 nC as the size of CSCY-TENG assembly increases from 9 to 36 cm^2. Similarly, the short-circuit current (I_{sc}) is also increased gradually from 2.7 μA to 5.1 μA (Fig. 4b). The effective contact area of CSCY-TENG can be enlarged readily by changing its length to some extent, resulting in improvement of output voltage. The reason is attributed to the larger the contact area of CSCY-TENG, and the more charges are generated[45]. And the CSCY-TENG assembly with a size of 36 cm^2 will be used in the following studies.

Considering that impact forces and frequencies on CSCY-TENG may vary in practical applications, the two factors have also been evaluated for electrical output performance. Fig. 4c-f and Fig. S8 b-c in Supporting Information show that the electric outputs of are increased with the increase of impact force and frequency. Specifically, at a fixed

frequency of 4 Hz, when the impact force increases from 10 to 70 N, the voltage and Q_{sc} is gradually increased from 63 V/63 nC to 150 V/125 nC and the I_{sc} is increased from 1.7 μA to 6.1 μA (Fig. 4c-d and Fig. S8b in Supporting Information). Similarly, at a fixed impact force of 70 N, the voltage, Q_{sc} and I_{sc} of CSCY-TENGs will be increased from 137 V/73 nC/3.7 μA to 174 V/126 nC/7.5 μA, as the impact frequency increases from 1 Hz to 5 Hz (Fig. 4e-f and Fig. S8c in Supporting Information). The reasons can be explained as follows: under a certain force, a higher impact frequency can stimulate the flow of external electrons in a shorter time and the surface charge of the friction layer will not be completely neutralized at an elevated frequency, which may result in an increased output[46-48]. Moreover, the output of the TENG increases with increased impact forces could be attributed to the more intimate contact between the N-ccsys and P-ccsys of CSCY-TENG at a larger magnitude of applied impact force[34].

As shown in Fig. 4g–h, the electric energy output of CSCY-TENG has also been systematically studied by connecting with external resistances. At a fixed frequency of 5 Hz and impact force of 70 N, different resistors from 1 KΩ to 500 MΩ are externally connected to test the output voltage and current. It can be seen that output current decreases with the increase of load resistance, while the voltage shows an opposite trend, which follows the Ohm's law. Peak power density and average power density[49, 50] reach the maximum value of 275 mW/m^2 and 57 mW/m^2 at a load resistance of 50 MΩ, respectively, as shown in Fig. 4h.

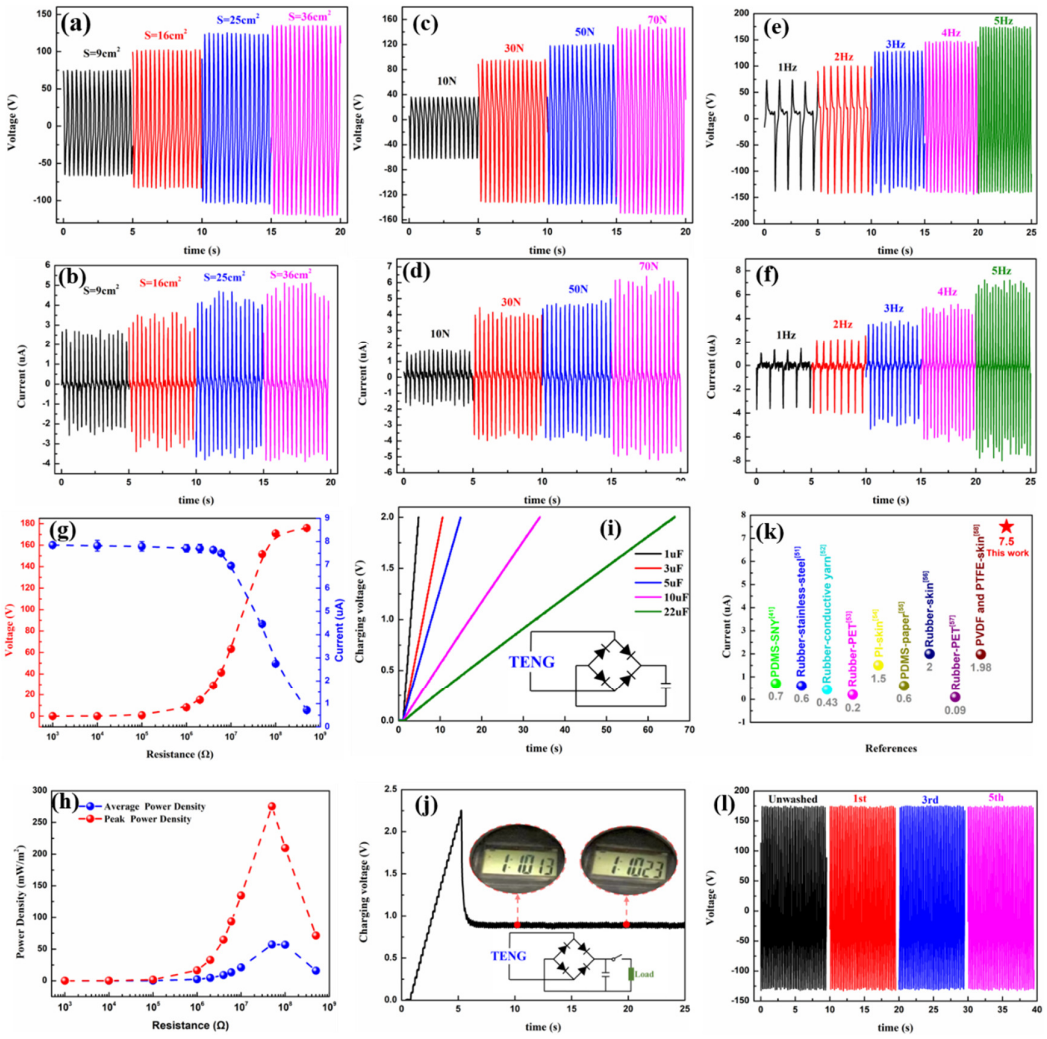

Fig. 4 (a) Output voltage and (b) short-circuit current of the CSCY-TENG with different sizes under the same impact force of 50 N and frequency of 4 Hz. (c) Output voltage and (d) short-circuit current of the CSCY-TENG with different impacting forces under the same size of 36 cm^2 and frequency of 4Hz. (e) Output voltage and (f) short-circuit current of the CSCY-TENG with different frequencies under the same size of 36 cm^2 and impact force of 70 N. (g) Dependence of the output voltage and current of the CSCY-TENG on load resistances. (h) Dependence of the instantaneous power density and average power density of the CSCY-TENG on load resistances. (i) Charging curves of 1 μF, 3 μF, 5 μF, 10 μF and 22 μF capacitors charged by the CSCY-TENG, and inset is the charging circuit diagram. (j) Charging voltage curves of the CSCY-TENG in the process of continuous powering electronic devices. The inserts are the photos of electronic devices under the continuous operational state. (k) Comparison of output electric current of CSCY-TENG and previous works. (l) Electric performance of the CSCY-TENG before and after washing for different times.

Next, the charging capacity of CSCY-TENG has been studied (Fig. 4i) by charging different values of capacitors, ranging from 1 μF to 22 μF. For 1 μF capacitor, it takes

about 4.8 s to be charged to 2 V while a 22 μF capacitor takes 66 s. Based on the charging time, charging rate of the capacitor can be calculated as 0.4 V/s for 1 μF, 0.2 V/s for 3 μF, 0.13 V/s for 5 μF, 0.06 V/s for 10 μF and 0.03 V/s for 22 μF, respectively. As a demonstration, the energy continuously generated by CSCY-TENG can be used to directly drive the electronic watch or other low-power electronics. Fig. 4j shows the corresponding charging voltage when the watch is working continuously, where the insets are the charging circuit and the electronic watch running continuously for 10 s. (see Video 4 in Supporting Information). As compared with previous works, our CSCY-TENG reveals a comparable and even higher electrical performance (Fig. 4k, S9 and Table S1 in Supporting Information)[41, 51-58]. Moreover, washability and stability are also the important requirements of textiles in practical applications. In order to study the performance after washing, CSCY-TENG is scrubbed by hand with commercial detergent in water like common textiles. The electrical performance is shown in Fig. 4l. It turns out that the electrical output of CSCY-TENG remains stable even after 5 times of washing. Furthermore, to investigate the mechanical property, the tensile and compression cycling tests of CSCY-TENG were also performed under an applied force. After 10 cycles of tensile (20%) and compression (50%) tests, CSCY-TENG demonstrates a stable mechanical property (see Fig. S10 in Supporting Information).

Owing to its good flexibility, washability and easy triggering, CSCY-TENG has potential applications in energy harvesting and bio-motion sensing. In order to study the electric performance, the single CSCY-TENG with a length of about 23 cm (Fig. 5a-f and Fig. S11 a-f in Supporting Information) and the CSCY-TENG assembly (Fig. 5g-n and Fig. S11 g-n in Supporting Information) with size of 36 cm^2 are deformed into various shapes and also fixed in different positions of the human body for investigation. Fig. 5a-c and Fig. S11a-c show that CSCY-TENG is versatile in generating electricity because various kinds of deformations can generate electricity, including stretching (Fig. 5a and Fig. S11a), twisting (Fig. 5b and Fig. S11b) and pressing (Fig. 5c and Fig. S11c). The corresponding voltage/Q_{sc} can reach about 2 V/3 nC, 8 V/9 nC and 10 V/15 nC, respectively. The CSCY-TENG can also be sewn on clothes to harvest energy in different positions of the human body. Fig. 5 d-f and Fig. S11 d-f shows that the CSCY-TENG is fixed on the human knee, elbow and the inside of the arm, respectively. Under repeated bending the knee and elbow and rubbing the arm, the CSCY-TENG exhibited a voltage/Q_{sc} about 6 V/3 nC. As showed in Fig. 5g-l and Fig. S11 g-l, when the CSCY-

TENG assembly with a size of 36 cm^2 is fixed to different positions of the human body for energy harvesting, such as the elbow joint, inside of the arm and knee joint, the voltage/Q_{sc} delivers 10 V/11 nC, 40 V/30 nC and 32 V/60 nC, respectively. The CSCY-TENG shown in Fig. 5j and Fig. S11j is fixed to inside of the arm, and electrical output mainly depends on the certain pressure on the CSCY-TENG caused by the swing of the arm, which is greater than that of the tension during the inward bending of the elbow joint of Fig. 5h and Fig. S11h. So it can realize a more efficient contact-separation motion during the swing of the arm, thus producing greater electrical outputs. In addition, the CSCY-TENG could also be laid under the foot to harvest energy from footsteps (Fig. 5m-n and Fig. S11m-n), The voltage under a normal walking can reach 100 V/110 nC. Owing to its unique structure, CSCY-TENG can be used for different applications. CSCY-TENG is basically a one-dimensional composite TENG, so it can be flexibly combined with fabrics or incorporated with the movement positions of the human body. In addition, the CSCY-TENG assembly with a slightly larger area, such as 36 cm^2, can be fixed at the joints to monitor human movement in real time. When the wearer suddenly falls, it can trigger a mobile phone alarm through signal detection. This is similar to the principle of anti-theft alarm carpet, which will be further discussed in Fig. 6.

As shown in Fig. 6, as demonstration of application, an anti-theft alarm carpet which can monitor signals and a wearable shoe for energy harvesting are designed with CSCY-TENGs. Fig. 6a shows the application of CSCY-TENG as an anti-theft alarm blanket. When someone steps on the carpet, CSCY-TENG will produce an output signal and transmit it to the mobile phone via wireless of Bluetooth. The mobile phone receives the signal and emits a ring as a reminder (see Video 5 and Video 6 in Supporting Information). And CSCY-TENG can also perform wireless alarm or LED flashing through the Android master-slave board (see Video 7 in Supporting Information). To explore the water tolerance of CSCY-TENG for its practical application potential, 0.1 g, 0.2 g and 0.3 g of water droplets were sprayed on the surface and then the Q_{sc} was recorded. After spraying water droplets, the Q_{sc} of the CSCY-TENG decreases first and then increases slowly. It takes only 3 min, 5 min and 10 min for the spray water weight of 0.1 g, 0.2 g and 0.3 g to return to the original Q_{sc}, respectively (see Fig. S12 in Supporting Information). Therefore, CSCY-TENG can be endowed with good humidity resistance and water tolerance.

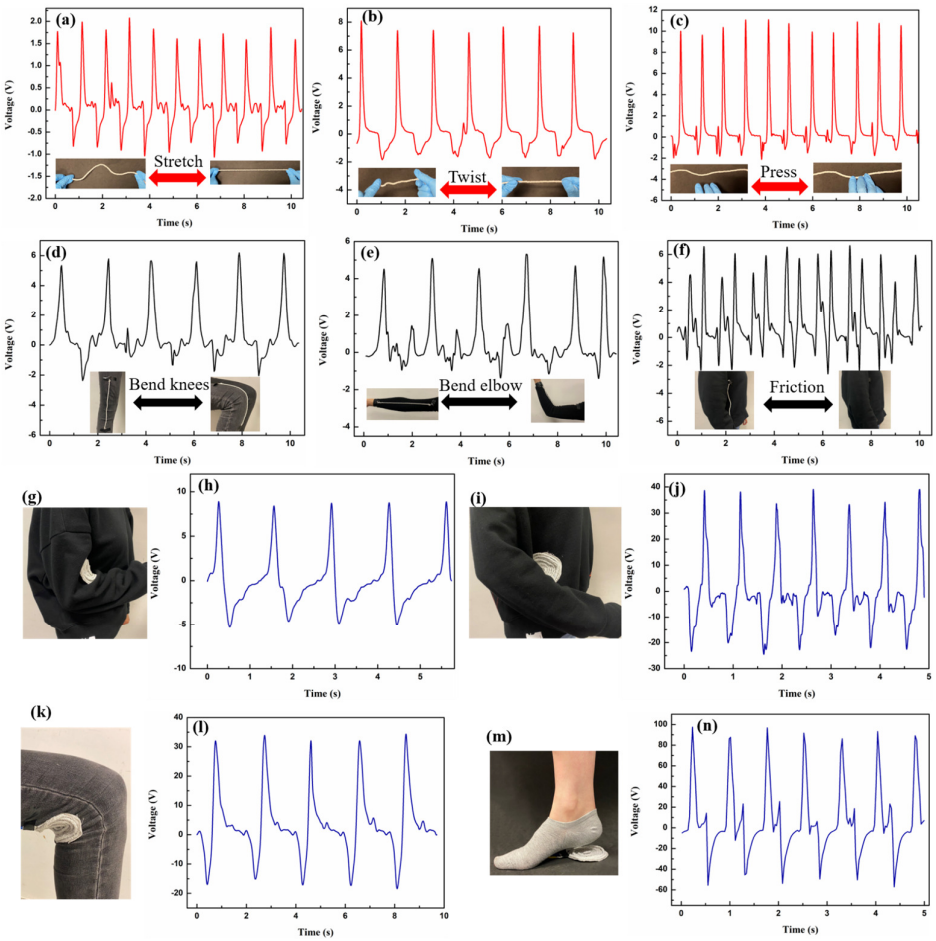

Fig. 5 Photograph and output voltage of the CSCY-TENG at different deformation shapes and positions of human body. (a) Stretched status. (b) Twisted status. (c) Pressed status. (d) Bend knees. (e) Bend elbow. (f) Arm friction (g-h) At the elbow joint. (i-j) Under the arm. (k-l) At the knee joint. (m-n) Under the foot.

Furthermore, the output power generated by CSCY-TENG can light up over 200 LEDs connected in series by a single impact on the area of 36 cm^2 as shown in Fig. 6b (see Video 8 in Supporting Information). To harvest the kinetic energy of people walking, a sustainable energy harvesting shoe is designed and directly driven by CSCY-TENG as the energy harvesting insoles. People can drive more than 78 LEDs when walking normally (see Video 9 in Supporting Information). It is suitable for night runners, mountain climbers and cyclists, and can also play a role of decoration, lighting or warning. To demonstrate that the CSCY-TENG can power commercial electronic devices, it was used for driving a commercial electrical calculator by CSCY-TENG. Fig. 6d shows the equivalent circuit of a self-powered system including CSCY-TENG, a capacitor of 22 μF, and a rectifier, which can drive a commercial electronic calculator to operate normally. The charging voltage of the capacitor increases rapidly from 0 to

2 V within 75s by tapping CSCY-TENGs continuously at a fixed frequency of 5 Hz and impact force of 70 N (Fig. 6e). And then Fig. 6f shows the electronic calculator was successfully driven (see Video S10 in Supporting Information).

Although our CSCY-TNEG has exhibited good potential in multifunctional wearable T-TENG, there is still room for improvement in practical applications. For example, production efficiency and electrical outputs can be further improved. At present, the improvement of mass-production efficiency is mainly depended on the development of triboelectric material coating integration. There is still much room for improvement in practical applications, which can be achieved by extending the reaction chamber or increasing the heating temperature. As for the electrical outputs, the power density, intrinsic impedance, and energy conversion efficiency of CSCY-TNEG should be further optimized by screening appropriate materials, designing structures, and employing power management circuits[59-61]. In the future, our research of CSCY-TENG will mainly focus on the improvement of energy conversion efficiency and production efficiency.

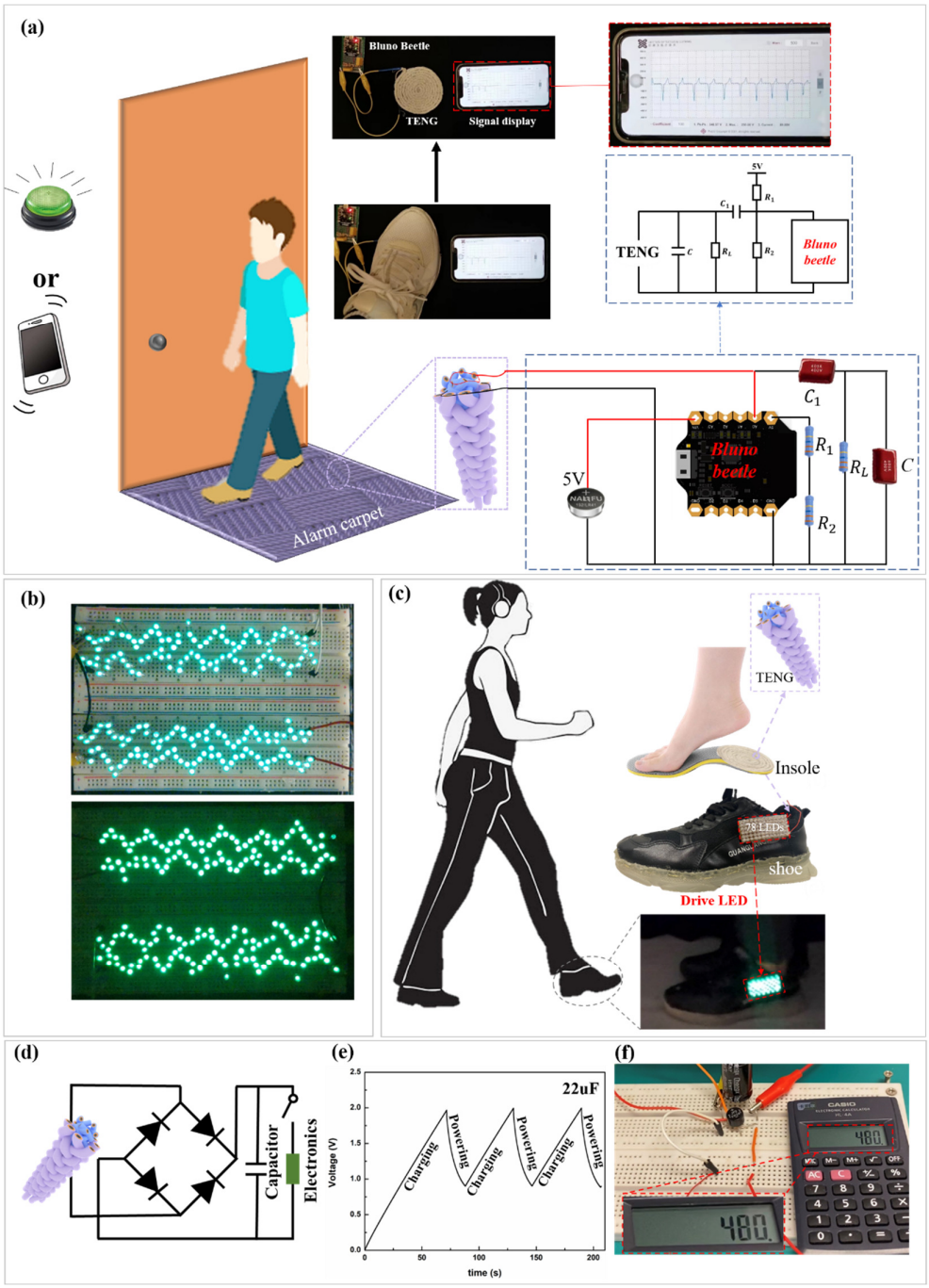

Fig. 6 (a) Schematic diagram of anti-theft alarm carpet. (b) Lighting up 200 LEDs under different light environment. (c) Schematic diagram of wearable and sustainable energy harvesting shoes. (d) The equivalent circuit for charging/discharging of electronics. (e) The charging/discharging curves of a commercial capacitor connected with CSCY-TENG for intermittently powering a commercial calculator. (f) The photographs of a commercial electrical calculator powered by CSCY-TENG.

3. Conclusion

In summary, core–spun coating yarn-based triboelectric nanogenerators with hierarchical structure is designed and fabricated, which are compatible with commercial spinning machine technology, braiding machine technology and continuous coating machine technology. For the core-spun yarns, SNY serves as the electrode core and cotton fibers serve as base shell materials for absorbing/coating with good triboelectric materials. Then nylon and doped PDMS coated core-spun yarns are used as positive and negative triboelectric materials and combined to obtain CSCY-TENG with hierarchical structure. Under a load frequency of 5 Hz and an applied force of 70 N, CSCY-TENG can achieve an output voltage of 174 V, and a peak power density and an average power density of 275 mW/m^2 and 57 mW/m^2, respectively. The energy can charge various commercial capacitors and power low-power electronics. CSCY-TENG can also be used as a domestic carpet with an anti-theft alarm function, and it can also be used as energy harvesting insoles to light and warn for night runners or mountain climbers. What's more, the CSCY-TENG can be traditionally washed and it is compatible with industrial-scale textile manufacturing. All these advantages of CSCY-TENG show their great potentials for viable applications in wearable electronics or smart textiles in the near future.

Experiment section

Materials

Nylon was purchased from Shenma Group Co., Ltd., China. Silver-plated nylon yarn (280D) was purchased from Qingdao Hengtong X-Silver Speciality Textile Co., Ltd., China. Cotton roving (400 Tex) was purchased from Shandong Zhongxian Textile Technology Co., Ltd., China. Formic acid (88–91%, ACS reagent) was purchased from Sigma-Aldrich. PDMS (Sylgard 184) was obtained from Dow Corning. $BaTiO_3$ (cubic crystalline phase, <100 nm particle size) was supplied by Aladdin (China). All the materials were used as received without any further purification.

Fabrication of the core-spun yarns

The core-spun yarns were fabricated by spinning technology using a ring spinning machine with additional of tension and filament guide devices. The fabrication process of core–spun yarn can be described briefly as: the SNY yarn passing through the tension

device and filament guide was stretched with a certain degree of tensile force, and its position was adjusted to be in the middle of core-spun yarn, forming the conductive SNY core of core-spun yarn. The cotton roving was fed through the bell mouth, drawn into short cotton fibers by the drafting rollers of ring spinning machine, and finally they wrapped onto the surface of SNY to form the shell layer of cotton fibers of the core-spun yarn.

Fabrication of the CSCY-TENG

Fabrication of N-ccsy: a solution of nylon (15 wt%) was prepared by dissolving nylon pellets in formic acid by continuous stirring for 2 h at a temperature of 70 °C. Core-spun yarn was coated with nylon by a coating machine when the yarn is passing through the liquid bath, as schematically illustrated in Fig. 2b, with a moving speed of 2 m/min. The formic acid was completely volatilized in the process of coating and N-CCSY was obtained. Environmental temperature and relative humidity are 22 ± 2 °C and 65 ± 5%, respectively.

Fabrication of P-ccsys: the PDMS@$BaTiO_3$ was prepared by adding PDMS base and curing agent at a ratio of 10:1, and then 10 wt% $BaTiO_3$was added to the PDMS mixed liquid. After stirring for 3 min, it was kept at room temperature for 30 min to remove the bubbles. The temperature of the coating machine was adjusted to 200±5° with other parameters the same as those for N-ccsy.

Braiding of the CSCY-TENG: First, 6 N-ccsys were braided together to form as the core of CSCY-TENG on a braiding technology and then removed from the machine. Then, the braided N-ccsys were taken as the core and re-feeded from the middle of the machine, and two PVA roving were braided as the middle layer. Afterwards, 8 P-ccsys were braided to the PVA surface as the shell. Finally, PVA was dissolved in warm water of about 50° to form CSCY-TENG with a hierarchical structure.

Characterizations and measurements

Electrical output performance of CSCY-TENG were evaluated by Keyboard Life Tester (ZXA03) under different impact forces and frequencies.The force signal was monitored by DAQ (Dewetron, Dewe-2600 DAQ system) at the same time. An electrometer (Keithley 6514) recorded the output voltage and shortcircuit current signals. The washability test of CSCY-TENG was referring to AATCC standard 135. SEM (Hitachi TM-3000) was employed to observe the structure of films.

Acknowledgements

The authors would like to acknowledge the funding support from the Research Grants Council of the Hong Kong Special Administrative Region, China (Project No. PolyU 15209020) for the work reported here.

References

[1] J. Wen, B. Xu, J. Zhou, Y. Chen, Novel high-performance asymmetric supercapacitors based on nickel-cobalt composite and PPy for flexible and wearable energy storage. Journal of Power Sources, 402 (2018) 91-98.

[2] K. Dong, X. Peng, Z.L. Wang, Fiber/fabric-based piezoelectric and triboelectric nanogenerators for flexible/stretchable and wearable electronics and artificial intelligence. Advanced Materials, 32 (2020) 1902549.

[3] Y. Chen, B. Xu, J. Gong, J. Wen, T. Hua, C.-W. Kan, J. Deng, Design of high-performance wearable energy and sensor electronics from fiber materials. ACS applied materials & interfaces, 11 (2018) 2120-2129.

[4] Y. Chen, Y. Cheng, Y. Jie, X. Cao, N. Wang, Z.L. Wang, Energy harvesting and wireless power transmission by a hybridized electromagnetic–triboelectric nanogenerator. Energy & Environmental Science, 12 (2019) 2678-2684.

[5] X. Guan, B. Xu, J. Gong, Hierarchically architected polydopamine modified BaTiO3@ P (VDF-TrFE) nanocomposite fiber mats for flexible piezoelectric nanogenerators and self-powered sensors. Nano Energy, 70 (2020) 104516.

[6] A. Nozariasbmarz, H. Collins, K. Dsouza, M.H. Polash, M. Hosseini, M. Hyland, J. Liu, A. Malhotra, F.M. Ortiz, F. Mohaddes, Review of wearable thermoelectric energy harvesting: From body temperature to electronic systems. Applied Energy, 258 (2020) 114069.

[7] F.-R. Fan, Z.-Q. Tian, Z.L. Wang, Flexible triboelectric generator. Nano energy, 1 (2012) 328-334.

[8] S. Niu, Z.L. Wang, Theoretical systems of triboelectric nanogenerators. Nano Energy, 14 (2015) 161-192.

[9] R. Hinchet, H.-J. Yoon, H. Ryu, M.-K. Kim, E.-K. Choi, D.-S. Kim, S.-W. Kim, Transcutaneous ultrasound energy harvesting using capacitive triboelectric technology. Science, 365 (2019) 491-494.

[10] X. Peng, K. Dong, C. Ye, Y. Jiang, S. Zhai, R. Cheng, D. Liu, X. Gao, J. Wang, Z.L. Wang, A breathable, biodegradable, antibacterial, and self-powered electronic skin

based on all-nanofiber triboelectric nanogenerators. Science Advances, 6 (2020) eaba9624.
[11] W. Paosangthong, R. Torah, S. Beeby, Recent progress on textile-based triboelectric nanogenerators. Nano Energy, 55 (2019) 401-423.
[12] X. Pu, Textile Triboelectric Nanogenerators for Energy Harvesting. Flexible and Wearable Electronics for Smart Clothing, (2020) 67-86.
[13] T. Busolo, P.K. Szewczyk, M. Nair, U. Stachewicz, S. Kar-Narayan, Triboelectric Yarns with Electrospun Functional Polymer Coatings for Highly Durable and Washable Smart Textile Applications. ACS Applied Materials & Interfaces, (2021).
[14] J. Gong, B. Xu, X. Guan, Y. Chen, S. Li, J. Feng, Towards truly wearable energy harvesters with full structural integrity of fiber materials. Nano Energy, 58 (2019) 365-374.
[15] X. Fan, N. Wang, J. Wang, B. Xu, F. Yan, Highly sensitive, durable and stretchable plastic strain sensors using sandwich structures of PEDOT: PSS and an elastomer. Materials Chemistry Frontiers, 2 (2018) 355-361.
[16] Q. Shi, T. He, C. Lee, More than energy harvesting–Combining triboelectric nanogenerator and flexible electronics technology for enabling novel micro-/nano-systems. Nano Energy, 57 (2019) 851-871.
[17] J. Zhong, Y. Zhang, Q. Zhong, Q. Hu, B. Hu, Z.L. Wang, J. Zhou, Fiber-based generator for wearable electronics and mobile medication. ACS nano, 8 (2014) 6273-6280.
[18] S. Jung, J. Lee, T. Hyeon, M. Lee, D.H. Kim, Fabric-based integrated energy devices for wearable activity monitors. Advanced Materials, 26 (2014) 6329-6334.
[19] T. Zhou, C. Zhang, C.B. Han, F.R. Fan, W. Tang, Z.L. Wang, Woven structured triboelectric nanogenerator for wearable devices. ACS applied materials & interfaces, 6 (2014) 14695-14701.
[20] X. Pu, L. Li, H. Song, C. Du, Z. Zhao, C. Jiang, G. Cao, W. Hu, Z.L. Wang, A self-charging power unit by integration of a textile triboelectric nanogenerator and a flexible lithium-ion battery for wearable electronics. Advanced Materials, 27 (2015) 2472-2478.
[21] Z. Tian, J. He, X. Chen, T. Wen, C. Zhai, Z. Zhang, J. Cho, X. Chou, C. Xue, Core–shell coaxially structured triboelectric nanogenerator for energy harvesting and motion sensing. RSC advances, 8 (2018) 2950-2957.
[22] Z. Zhao, C. Yan, Z. Liu, X. Fu, L.M. Peng, Y. Hu, Z. Zheng, Machine-washable textile triboelectric nanogenerators for effective human respiratory monitoring through loom weaving of metallic yarns. Advanced Materials, 28 (2016) 10267-10274.

[23] W. Seung, M.K. Gupta, K.Y. Lee, K.-S. Shin, J.-H. Lee, T.Y. Kim, S. Kim, J. Lin, J.H. Kim, S.-W. Kim, Nanopatterned textile-based wearable triboelectric nanogenerator. ACS nano, 9 (2015) 3501-3509.
[24] Y.-T. Jao, P.-K. Yang, C.-M. Chiu, Y.-J. Lin, S.-W. Chen, D. Choi, Z.-H. Lin, A textile-based triboelectric nanogenerator with humidity-resistant output characteristic and its applications in self-powered healthcare sensors. Nano Energy, 50 (2018) 513-520.
[25] Z. Yuan, T. Zhou, Y. Yin, R. Cao, C. Li, Z.L. Wang, Transparent and flexible triboelectric sensing array for touch security applications. Acs Nano, 11 (2017) 8364-8369.
[26] W. Weng, P. Chen, S. He, X. Sun, H. Peng, Smart electronic textiles. Angewandte Chemie International Edition, 55 (2016) 6140-6169.
[27] M. Liu, X. Pu, C. Jiang, T. Liu, X. Huang, L. Chen, C. Du, J. Sun, W. Hu, Z.L. Wang, Large-area all-textile pressure sensors for monitoring human motion and physiological signals. Advanced materials, 29 (2017) 1703700.
[28] S.S. Kwak, H. Kim, W. Seung, J. Kim, R. Hinchet, S.-W. Kim, Fully stretchable textile triboelectric nanogenerator with knitted fabric structures. ACS nano, 11 (2017) 10733-10741.
[29] X. Pu, M. Liu, X. Chen, J. Sun, C. Du, Y. Zhang, J. Zhai, W. Hu, Z.L. Wang, Ultrastretchable, transparent triboelectric nanogenerator as electronic skin for biomechanical energy harvesting and tactile sensing. Science advances, 3 (2017) e1700015.
[30] A.Y. Choi, C.J. Lee, J. Park, D. Kim, Y.T. Kim, Corrugated textile based triboelectric generator for wearable energy harvesting. Scientific reports, 7 (2017) 1-6.
[31] J. Li, B. Xu, Novel highly sensitive and wearable pressure sensors from conductive three-dimensional fabric structures. Smart Materials and Structures, 24 (2015) 125022.
[32] Z. Zhao, Q. Huang, C. Yan, Y. Liu, X. Zeng, X. Wei, Y. Hu, Z. Zheng, Machine-washable and breathable pressure sensors based on triboelectric nanogenerators enabled by textile technologies. Nano Energy, 70 (2020) 104528.
[33] C.S. Boland, U. Khan, G. Ryan, S. Barwich, R. Charifou, A. Harvey, C. Backes, Z. Li, M.S. Ferreira, M.E. Möbius, Sensitive electromechanical sensors using viscoelastic graphene-polymer nanocomposites. Science, 354 (2016) 1257-1260.
[34] X. Guan, B. Xu, M. Wu, T. Jing, Y. Yang, Y. Gao, Breathable, washable and wearable woven-structured triboelectric nanogenerators utilizing electrospun nanofibers for biomechanical energy harvesting and self-powered sensing. Nano

Energy, 80 (2021) 105549.
[35] J. Wen, B. Xu, Y. Gao, M. Li, H. Fu, Wearable Technologies Enable High-performance Textile Supercapacitors with Flexible, Breathable and Wearable Characteristics for Future Energy Storage. Energy Storage Materials, (2021).
[36] Y. Mao, Y. Li, J. Xie, H. Liu, C. Guo, W. Hu, Triboelectric nanogenerator/supercapacitor in-one self-powered textile based on PTFE yarn wrapped PDMS/MnO2NW hybrid elastomer. Nano Energy, 84 (2021) 105918.
[37] A. Yu, X. Pu, R. Wen, M. Liu, T. Zhou, K. Zhang, Y. Zhang, J. Zhai, W. Hu, Z.L. Wang, Core–Shell-Yarn-Based Triboelectric Nanogenerator Textiles as Power Cloths. ACS Nano, 11 (2017) 12764-12771.
[38] Y.C. Lai, J. Deng, S.L. Zhang, S. Niu, H. Guo, Z.L. Wang, Single-thread-based wearable and highly stretchable triboelectric nanogenerators and their applications in cloth-based self-powered human-interactive and biomedical sensing. Advanced Functional Materials, 27 (2017) 1604462.
[39] L. Ma, M. Zhou, R. Wu, A. Patil, H. Gong, S. Zhu, T. Wang, Y. Zhang, S. Shen, K. Dong, Continuous and scalable manufacture of hybridized nano-micro triboelectric yarns for energy harvesting and signal sensing. ACS nano, 14 (2020) 4716-4726.
[40] K. Dong, J. Deng, Y. Zi, Y.C. Wang, C. Xu, H. Zou, W. Ding, Y. Dai, B. Gu, B. Sun, 3D orthogonal woven triboelectric nanogenerator for effective biomechanical energy harvesting and as self-powered active motion sensors. Advanced Materials, 29 (2017) 1702648.
[41] K. Dong, X. Peng, J. An, A.C. Wang, J. Luo, B. Sun, J. Wang, Z.L. Wang, Shape adaptable and highly resilient 3D braided triboelectric nanogenerators as e-textiles for power and sensing. Nature communications, 11 (2020) 1-11.
[42] E. He, Y. Sun, X. Wang, H. Chen, B. Sun, B. Gu, W. Zhang, 3D angle-interlock woven structural wearable triboelectric nanogenerator fabricated with silicone rubber coated graphene oxide/cotton composite yarn. Composites Part B: Engineering, 200 (2020) 108244.
[43] X. He, Y. Zi, H. Guo, H. Zheng, Y. Xi, C. Wu, J. Wang, W. Zhang, C. Lu, Z.L. Wang, A highly stretchable fiber-based triboelectric nanogenerator for self-powered wearable electronics. Advanced Functional Materials, 27 (2017) 1604378.
[44] S. Niu, Y. Liu, S. Wang, L. Lin, Y.S. Zhou, Y. Hu, Z.L. Wang, Theoretical investigation and structural optimization of single-electrode triboelectric nanogenerators. Advanced Functional Materials, 24 (2014) 3332-3340.
[45] S. Niu, S. Wang, L. Lin, Y. Liu, Y.S. Zhou, Y. Hu, Z.L. Wang, Theoretical study of

contact-mode triboelectric nanogenerators as an effective power source. Energy & Environmental Science, 6 (2013) 3576-3583.
[46] Q. Ye, Y. Wu, Y. Qi, L. Shi, S. Huang, L. Zhang, M. Li, W. Li, X. Zeng, H. Wo, X. Wang, S. Dong, S. Ramakrishna, J. Luo, Effects of liquid metal particles on performance of triboelectric nanogenerator with electrospun polyacrylonitrile fiber films. Nano Energy, 61 (2019) 381-388.
[47] J. Shen, Z. Li, J. Yu, B. Ding, Humidity-resisting triboelectric nanogenerator for high performance biomechanical energy harvesting. Nano Energy, 40 (2017) 282-288.
[48] X.-S. Zhang, M.-D. Han, R.-X. Wang, F.-Y. Zhu, Z.-H. Li, W. Wang, H.-X. Zhang, Frequency-multiplication high-output triboelectric nanogenerator for sustainably powering biomedical microsystems. Nano letters, 13 (2013) 1168-1172.
[49] X. Yang, L. Xu, P. Lin, W. Zhong, Y. Bai, J. Luo, J. Chen, Z.L. Wang, Macroscopic self-assembly network of encapsulated high-performance triboelectric nanogenerators for water wave energy harvesting. Nano Energy, 60 (2019) 404-412.
[50] P. Rui, W. Zhang, Y. Zhong, X. Wei, Y. Guo, S. Shi, Y. Liao, J. Cheng, P. Wang, High-performance cylindrical pendulum shaped triboelectric nanogenerators driven by water wave energy for full-automatic and self-powered wireless hydrological monitoring system. Nano Energy, 74 (2020) 104937.
[51] W. Gong, C. Hou, J. Zhou, Y. Guo, W. Zhang, Y. Li, Q. Zhang, H. Wang, Continuous and scalable manufacture of amphibious energy yarns and textiles. Nature communications, 10 (2019) 1-8.
[52] K. Dong, J. Deng, W. Ding, A.C. Wang, P. Wang, C. Cheng, Y.C. Wang, L. Jin, B. Gu, B. Sun, Versatile core–sheath yarn for sustainable biomechanical energy harvesting and real-time human-interactive sensing. Advanced Energy Materials, 8 (2018) 1801114.
[53] C. Chen, L. Chen, Z. Wu, H. Guo, W. Yu, Z. Du, Z.L. Wang, 3D double-faced interlock fabric triboelectric nanogenerator for bio-motion energy harvesting and as self-powered stretching and 3D tactile sensors. Mater. Today, 32 (2020) 84-93.
[54] L. Ma, R. Wu, S. Liu, A. Patil, H. Gong, J. Yi, F. Sheng, Y. Zhang, J. Wang, J. Wang, A Machine-Fabricated 3D Honeycomb-Structured Flame-Retardant Triboelectric Fabric for Fire Escape and Rescue. Advanced materials, 32 (2020) 2003897.
[55] C. Jiang, X. Li, Y. Ying, J. Ping, A multifunctional TENG yarn integrated into agrotextile for building intelligent agriculture. Nano Energy, 74 (2020) 104863.
[56] K. Dong, Z. Wu, J. Deng, A.C. Wang, H. Zou, C. Chen, D. Hu, B. Gu, B. Sun, Z.L.

Wang, A stretchable yarn embedded triboelectric nanogenerator as electronic skin for biomechanical energy harvesting and multifunctional pressure sensing. Advanced Materials, 30 (2018) 1804944.
[57] L. Chen, C. Chen, L. Jin, H. Guo, A.C. Wang, F. Ning, Q. Xu, Z. Du, F. Wang, Z.L. Wang, Stretchable negative Poisson's ratio yarn for triboelectric nanogenerator for environmental energy harvesting and self-powered sensor. Energy & Environmental Science, 14 (2021) 955-964.
[58] Q. Qiu, M. Zhu, Z. Li, K. Qiu, X. Liu, J. Yu, B. Ding, Highly flexible, breathable, tailorable and washable power generation fabrics for wearable electronics. Nano Energy, 58 (2019) 750-758.
[59] C. Wu, A.C. Wang, W. Ding, H. Guo, Z.L. Wang, Triboelectric nanogenerator: a foundation of the energy for the new era. Advanced Energy Materials, 9 (2019) 1802906.
[60] X. Cheng, L. Miao, Y. Song, Z. Su, H. Chen, X. Chen, J. Zhang, H. Zhang, High efficiency power management and charge boosting strategy for a triboelectric nanogenerator. Nano Energy, 38 (2017) 438-446.
[61] J. Nie, X. Chen, Z.L. Wang, Electrically responsive materials and devices directly driven by the high voltage of triboelectric nanogenerators. Advanced Functional Materials, 29 (2019) 1806351.